UDC：539.26：666.1.056

In-situ Monitoring of Thermally Induced Resistivity Changes in Silver Thin Films

Barbara DE MAEYER*, Frédéric VAN WONTERGHEM, Joris PROOST***, Nicolas CLEMENT******

This study investigates the evolution of the microstructural properties under thermal treatments of silver thin films deposited by wet chemistry on a glass substrate. It aims to prove the link between microstructural and crystallographic changes on the basis of in-situ monitoring of electrical resistivity. The resistivity of the silver thin film decreases for thermal treatments performed between 110°C and 250°C. This decrease is explained by the elimination of crystallographic defects, highlighted by the decrease of the full width at half maximum (FHWM) of the XRD peaks, and by the inexistence of morphological changes on the same temperature interval. For thermal treatments performed at a temperature above 250°C, changes in FWHM and in resistivity are negligible. However, a change in microstructure appears through the formation of holes. Hole formation combined with the increase in the {111}/{200} ratio from 250°C on is explained by the initiation of an agglomeration phenomenon. The agglomeration phenomenon is thus independent from the resistivity changes occurring at a temperature lower than 320°C.

*Université Catholique de Louvain, barbara.demaeyer@uclouvain.be IMMC/IMAP-Place Sainte Barbe 2, 1348 Louvain-la-Neuve, Belgium
**Université Catholique de Louvain, frederic.vanwonterghem@uclouvain.be IMMC/IMAP-Place Sainte Barbe 2, 1348 Louvain-la-Neuve, Belgium
***Université Catholique de Louvain, joris.proost@uclouvain.be IMMC/IMAP-Place Sainte Barbe 2,1348 Louvain-la-Neuve, Belgium
****AGC Glass Europe, T&I nicolas.clement@eu.agc.com Rue de l'Aurore 2, 6040 Jumet, Belgium

Context of the research

Concentrated Solar Power (CSP) is an utility-scale solar energy technology using large mirror fields to concentrate the sunlight on a target, in order to produce supersaturated steam for power generation using a standard Rankine cycle. The technology requires a mirror area of roughly $7m^2$ per kW, resulting in huge mirror fields (e.g. 2.6 million square meters for the 370MW Ivanpah project)[(1)]. As a leading mirror producer, AGC could not let this opportunity pass by.

For the solar mirrors, three main challenges are to be faced. Firstly, investment cost is a strong limiting factor for this technology competing against well-established coal or nuclear power: the fabrication process must be quite optimized and use sparingly some expensive raw materials. Second, a durability longer than 20 years in harsh outdoor conditions must be reached, including resistance to sand storms, large temperature variations, intense and prolonged UV exposure[(2)]. And third, the performance level of the solar mirror – its ability to reflect the sun's energy onto the target, has to be increased well above the level of the average bathroom mirror[(3)].

The research paper resulting from a collaboration between AGC and the University of Louvain (UCL, Belgium) deals primarily with this last point. When you are already using the least absorbing glass as substrate, and the most reflective material -silver- as mirror coating, room for improvement mainly lies in the way this reflective material can be made even brighter. As reflectivity finds its roots in the mobility of the electrons, removing the hurdles to electron movement sounds like a nice idea. This can be accomplished for instance by providing thermal energy to the system, enabling it to reach a lower-energy, lower-defects state. The paper details how to observe directly the changes occurring in the silver film during annealing, and how parasitic effects like void formation or agglomeration can counteract the desired defect-removal process.

Ⅰ. Introduction

Silver, as thin film deposited on SiO_2 substrates, constitutes a potential interconnect material for its high resistance properties to electromigration and its capacity to reduce RC delay. Nevertheless, the low thermal stability of Ag deposited on SiO_2 substrates is a major issue for metallization[(4)(5)(6)]. Indeed, this instability is problematic because it entails an agglomeration phenomenon, thus increasing the electrical resistance by disrupting the film surface. Agglomeration is a mass transport process where the driving force is the minimization of the total free energy of the system[(4)]. The agglomeration process in silver films during thermal treatments has already been widely studied, with the aim to avoid or reduce it[(7)(8)]. For electrical applications, resistivity measurements have been carried out before and after thermal treatments to determine the effect of temperature. Some authors already commented on the reduction of resistivity depending on the annealing temperature[(7)(8)(9)]. They also showed important jumps of resistivity for higher annealing temperatures due to the loss of film continuity. These studies have shown that the phenomenon linked to those two changes in resistivity comes from recrystallization. However, most of those studies restrict to two deposition techniques: physical vapor deposition and evaporation. This work aims to extend those studies to another deposition type and using in-situ electrical resistivity measurement. It investigates the evolution of the microstructural properties of silver thin films deposited by wet chemistry on glass substrates under thermal treatments. It thereby aims to prove the link between microstructural and electrical resistivity changes on the basis of in-situ monitoring of the electrical resistivity.

Ⅱ. Experimental

Silver thin films with a thickness of 140 nm have been deposited on 950 μm thick glass substrates by a wet chemistry process at room pressure. The process, described by Schweig[(10)] consists in sensitization of the glass substrate by treating its surface with a solution of tin chloride (1 g/L) to accelerate the silver deposition and to improve the adhesion between silver and glass. In addition, an aqueous solution of $PdCl_2$ is sprayed after the tin chloride step due to its catalytic properties. The palladium solution is prepared by mixing 1 g of palladium chloride to 200 ml of hydrochloric acid and 800 ml of distilled water. The deposition of silver is obtained by the reduction of the $AgNO_3$ solution with a formaldehyde solution. The silver nitrate solution is produced using 100 g of $AgNO_3$ dissolved in 800 ml of distilled water and 200 ml of ammonia. This silver solution is sprayed onto the glass surface with a solution made up of 0.2 ml formaldehyde and 10 g of dextrose in 1000 ml of

distilled water. Another spray of stannous chloride is applied on silver with a solution similar to the one of the first step to create a protective layer to silver oxidation. The obtained coating layer consists in 0.45 nm of Sn as sensitizing layer, followed by clusters of Pd (mean thickness < 0.06 nm), 140 nm of silver and 0.45 nm of a Sn protective layer.

In-situ four point probe resistivity measurements were performed on a heating stage (LTS420 from LINKAM) under Argon atmosphere using an in line Van der Pauw configuration [6][8]. The films were annealed at 10 ℃/min to different maximum annealing temperatures ranging upto 320℃, maintained at those temperatures during 20 minutes, and finally freely let cooled down to room temperature. The indicated annealing temperatures represent the effective sample temperature, as obtained from separate calibration runs with a thermocouple attached to the Ag surface.

Scanning electron microscopy was used to observe morphological changes during the thermal treatments using a Zeiss Ultra55 field emission gun scanning electron microscope operating at 3 keV. In order to investigate changes in crystallographic texture as a function of annealing temperature, X-ray diffraction measurements were performed on as-deposited and annealed samples in Bragg-Brentano configuration with Co Kα radiation (θ/2θ scans in Bragg-Brentano configuration with Co Kα radiation), for 2θ going from 40° to 100°. The operating voltage and filament current were 40kV and 30mA, respectively.

Ⅲ. Results

A. Electrical properties

Fig.1 presents the measured resistivity evolution of a silver thin film as a function of temperature during annealing for both the heating and cooling steps, as well as a function of the maintained time at the maximum annealing temperature. The resistivity measurement was performed for two successive thermal treatments up to a maximum annealing temperature of 320℃.

The first observation arising from **Fig.1** is that, after the first annealing, the final resistivity at room temperature (1.66 μΩm) is lower than the initial resistivity (2.07 μΩm). No further change is observed for the resistivity after the first and second annealing.

The second observation is that, during the heating step for the first annealing, the resistivity shows three different regimes. Between 30℃ to 110° C, it rises with a Temperature Coefficient of Resistance (TCR) of 2.7 × 10^{-3}/℃. Above 110° C, the resistivity increase slows down up to 250° C with a TCR value of about 1.2 × 10^{-3}/℃. After this second regime, the resistivity rises again with a TCR of 2.4 × 10^{-3}/℃. The two cooling slopes and the heating slope of the second annealing are statistically identical with a value of (3.0±0.1) × 10^{-3}/℃. It is worth noting that the resistivity and its TCR of bulk silver at 20℃ are 1.63 μΩm and 3.8 x 10^{-3}/℃, respectively[11], slightly different to our measured values.

To complement the thermal treatment at 320℃, two additional thermal treatments have been carried out under the same conditions, but at a maximum annealing temperature of 110℃ and 250 ℃. Those temperatures correspond to the near-end of the first and second regime. **Fig.2** presents the resulting relative resistivity changes of the Ag thin films. During the heating step, the slope from 30℃ to 110℃ is statistically identical for all samples with a TCR of (2.5±0.2) × 10^{-3}/℃. Above 110℃, a change in slope is observed between the annealing conditions at 250℃ and 320 ℃, which is attributed to inhomogeneities existing

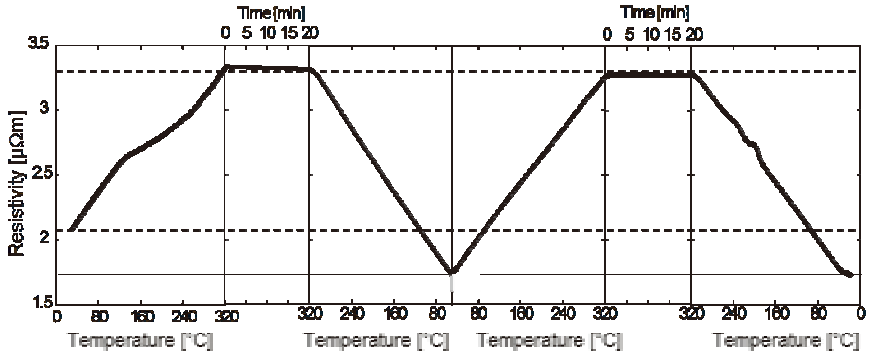

Fig.1 Evolution of the electrical resistivity of a Ag thin film on glass substrate as a function of annealing temperature and time.

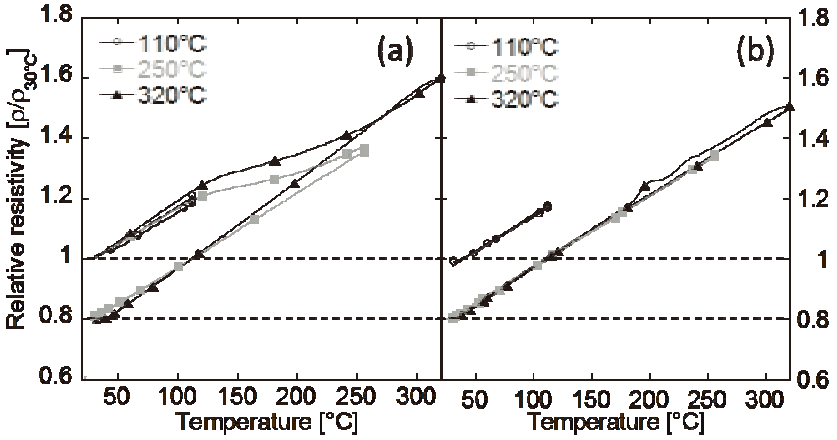

Fig.2 Electrical resistivity of silver as a function of temperature during a first (a), and second (b) annealing.

between different samples. Nonetheless, for these two samples, the first annealing process leads to the same decrease in resistivity of 21%. At 110℃, no significant change in resistivity is observed after the first and second annealing.

For annealing conditions ranging from 110℃ to 320℃, **Fig.3** shows that most of the resistivity decrease occurs between 110℃ and 250℃. No change in resistivity is observed for a maximum annealing temperature below 110℃. Above 250℃, the resistivity no longer changes. Moreover, a second annealing does not lead to any further resistivity decrease.

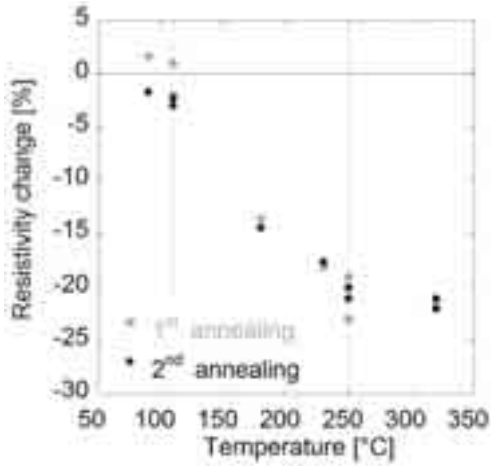

Fig.3 Electrical resistivity change of silver after thermal treatment as a function of the maximum annealing temperature for two successive annealings.

B. Crystallographic properties

X-ray diffractograms obtained from as-deposited and annealed silver samples at 110℃, 250℃ and 320℃ are shown in **Fig.4**. A global increase in peak intensity when increasing the annealing temperature is observed for all orientations.

Fig.5 shows the change of the {111}/{200} intensity ratio for different annealing temperatures after two identical successive thermal treatments. During the first annealing, the {111}/{200} ratio increases with temperature above 110℃. The second annealing does not lead to any further changes.

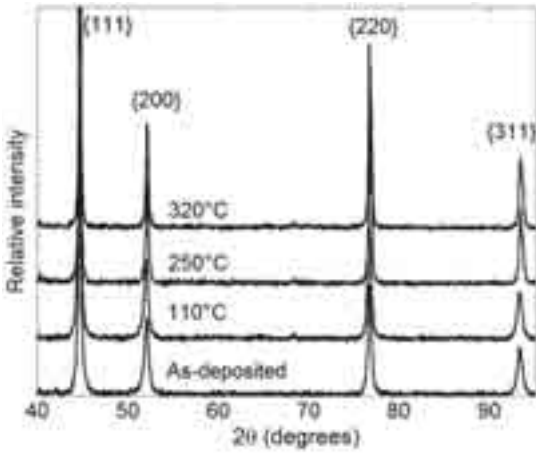

Fig.4 Bragg-Brentano XRD diffractograms obtained from silver thin films on glass substrates.

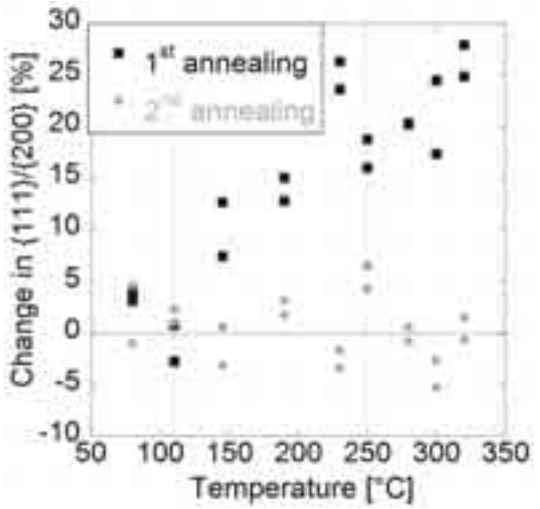

Fig.5 Change in {111}/{200} peak intensity ratio of silver thin films after two identical successive thermal treatments as a function of the maximum annealing temperature.

Concerning the {111} / {200} x-ray intensity ratio's for the as-deposited samples, **Fig.6** shows that this ratio is small compared to the one for films deposited by an evaporation technique taken from ref(8). However, as compared to an indexed silver powder[12], our Ag films do show a preferential {111} and {220} orientation.

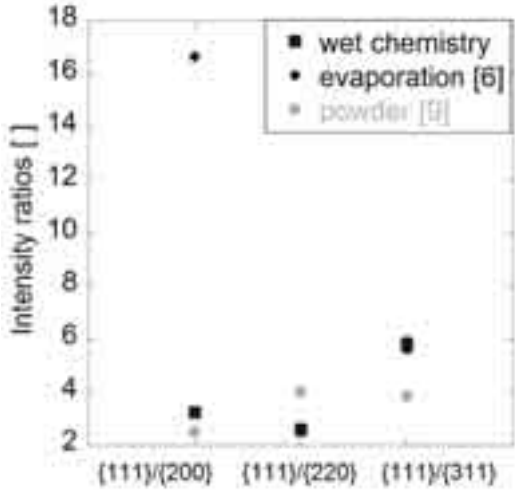

Fig.6 X-ray intensity ratios of as-deposited silver thin films on glass substrate deposited by wet chemistry compared to an evaporated silver thin film on a SiO_2 substrate[8] and to a randomly oriented powder[12].

The full width at half maximum (FWHM) of the {111} peak of as-deposited and annealed Ag thin films is reported in **Fig.7**. This graph points towards a significant decrease in the FWHM with increasing annealing temperature, most pronounced in the range between 110 and 250℃. This temperature range is the same as the one for which the second resistivity regime is observed during the first heating step. The maximum FWHM decrease observed at 250℃ is about 31%.

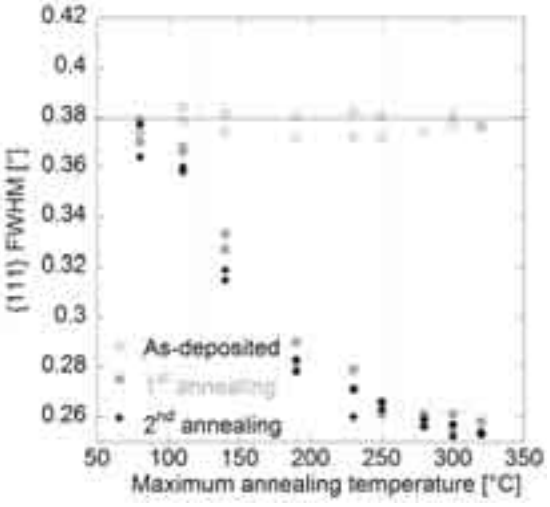

Fig.7 Full width at half maximum for as-deposited, first and second annealing as a function of the maximum annealing temperature.

It has to be noted that a similar behavior is obtained for FWHM of the {200}, {220} and {311} plane families. For the second annealing, no more changes in FWHM occur.

C. Morphological properties

Fig.8 presents changes in surface morphology of Ag thin films as a function of annealing temperature. The micrographs indicate the onset of void formation for thermal treatments up to 250℃. The size and the number of these voids increase with maximum annealing temperature, some reaching 1 μm^2 at 320℃. At the same time, no visible change in the size of the topological features occurs with increasing annealing temperatures.

Fig.9 presents a cross-section view of the silver film. Equiaxial grains are observed, with a size only slightly smaller than the thickness of the film. Therefore, it seems reasonable to assume that the grain size and surface morphological feature size are linked.

In addition to scanning electron microscopy, AFM imaging has been carried out as well. The mean roughness (RMS) values measured before and after annealing at 320℃ are 13±2 nm and 13±3 nm respectively, meaning that no significant change in surface roughness has occurred.

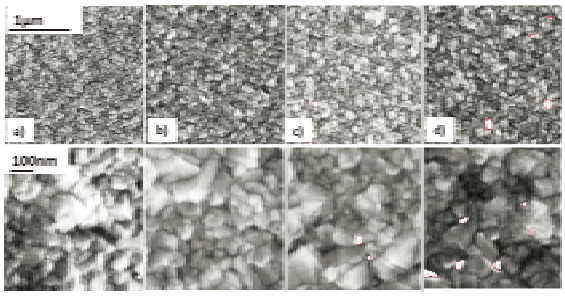

Fig.8 Scanning electron micrographs at different magnifications of Ag thin films on amorphous glass substrates (a) as-deposited, annealed up to (b) 110 ℃, (c) 250℃, (d) 320℃ for 20 minutes under argon. Voids are highlighted by white spots.

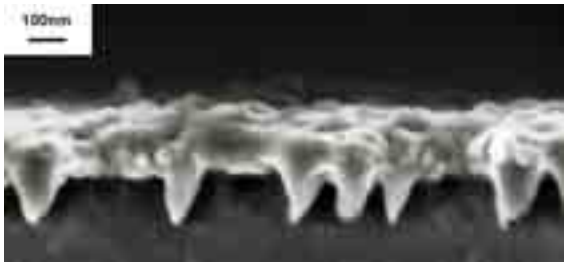

Fig.9 Scanning electron micrographs of Ag thin films on amorphous glass substrates, cross section view after breakage of the sample.

Ⅳ. Discussion

According to Matthiessens rule, the electrical resistivity of metallic thin films can be divided in three contributions[13]

$$\rho_f = \rho_T + \rho_S + \rho_G$$

where ρ_T represents is the electron/phonon interaction which is highly temperature dependent, ρ_S being the scattering of conduction electrons on structural defects line dislocations, vacancies, alloying elements and impurities and ρ_G a geometrical scattering component (e.g. at internal and external interfaces).

As seen in **Fig.1**, the resistivity curve during the heating cycle is characterized by three different regimes. In the first regime which ranges from 20 ℃ to 110℃, the TCR values are identical during the first and second annealing. Therefore, no irreversible processes take place in this temperature range, meaning that ρ_T dominates.

In the second regime, occurring between 110℃ to 250℃, the decrease in TCR is attributed to a decrease in ρ_S, which is the resistivity component influenced by the scattering of conduction electrons on structural defects. Above 110℃, the thermal energy is sufficient to initiate removal of structural defects, as reflected by a decrease in FWHM. Indeed, FWHM is inversely proportional to the apparent size of crystalline grains, the latter being largely influenced by the existence of crystalline defects[14]. Therefore, a lower FWHM reflects a lower degree of crystalline defects. The decrease in FWHM shown in **Fig.7** only occurs for a maximum annealing temperature ranging from 110℃ to 250℃, which is also the temperature range where the second resistivity regime occurs.

The SEM results (**Fig.8**) show no change in apparent grain size, whereas the XRD FWHM (**Fig.4**) decreases significantly. The absence of changes in the film morphology, as observed in **Fig.8**, suggests that no displacement of grain boundaries has occurred. Consequently, the measured decrease in FWHM is attributed to the annihilation of smaller 1D or punctual defects. This assumption is supported by **Fig.4**, showing that the intensity of the all the peaks has increased: there was no growth of some grains at the expense of others, but rather an elimination of defects resulting in larger X-Rays correlation length.

The defect removal is completed by 250℃, as no more decrease in FWHM occurs and the second annealing does not lead to further changes. This lack of significant change in FWHM correlates well with the absence of a slope change in resistivity during the second annealing.

In the third regime, the TCR increases again towards a same value which is very similar as the one for the first regime. Therefore, for this part of the slope, the temperature dependent electron-phonon interaction ρ_S can be assumed to dominate. Note that while a slight difference is being observed between the slopes of the first and the second regimes (2.7×10^{-3}/℃ and 2.4×10^{-3}/℃) during the first annealing. During the second annealing, this difference has disappeared, and all the three regimes present the same slope of 3.0×10^{-3}/℃.

At the same time, this part of the curve also corresponds to the onset of agglomeration, since the scanning electrons micrographs in **Fig.8** show formation of voids above 250℃, corresponding to the end of the second resistivity regime. However, the amount of voids is not sufficient yet to have a significant impact on the resistivity since the corresponding TCR-value is very close to the one for the first regime. Therefore, the resistivity evolution in the third regime does not permit to predict the onset of agglomeration. Agglomeration is a process occurring by the formation and growth of voids, thereby resulting in the exposure of the underlying substrate. Its driving force is determined by the balance of the film and substrate surface energies, the film/substrate interfacial energy, as well as the film strain energy [15]. Reduction of the interfacial energy is a key driving force for agglomeration. By assuming that the substrate surface energy is similar to that of amorphous SiO_2, its value is lower than that of silver ($\gamma_{Ag}/\gamma_{SiO2} \cong 4$[16][17][18][19][20] with γ_{Ag}=0.903 J/m^2). Moreover Kim et al.[8] have reported that the interfacial energy between silver and SiO_2 is higher than that of the substrate ($\gamma_{Ag/SiO2}$ =0.7 J/m^2; γ_{SiO2} =0.225 J/m^2). Agglomeration will thus occur to minimize the energy of the system by increasing the exposed substrate surface area.

In this work, no change in grain size (see **Fig.8**) and in roughness has been observed. Therefore, grain growth is not one of the driving forces in this system and another factor should play a role. Indeed, Alford et al.[21] have observed that the onset temperature of agglomeration has a strong underlayer dependence. The presence of Pd and Sn between the glass substrate and the silver film can change the onset temperature of agglomeration. In addition, it is seen in **Fig.5** that the

{111} / {200} ratio continues to increase above 250° C, whereas no further change in FWHM and in resistivity is observed above this temperature. This increase of the {111} / {200} ratio with temperature is consistent with the results obtained by Kim et al[8]. The amount of voids is not sufficient to have a significant impact on the resistivity. Literature results have shown that total disruption of the film occurs at temperatures of about 600℃ depending on the alloying elements, leading to an abrupt increase in resistivity[7][8][9][22][23][24]. In our case, one can imagine that the process of agglomeration has only been initiated at about 250℃, but will progress at higher temperatures leading to a further increase in {111} / {200} ratio and, eventually, in a TCR-increase. That will be then the part where the geometrical scattering component ρ_G will become dominant.

Ⅴ. Conclusions

In this paper, the evolution of the electrical resistivity of silver thin films deposited on glass substrates has been investigated as a function of temperature. Combining these results with SEM analysis, it has been highlighted that changes occurring during annealing in morphological, crystallographic and electrical properties are linked.

The final resistivity was found to decrease after thermal treatments performed between 110℃ and 320℃. This decrease is explained by the elimination of intragranular defects, evidenced by a decrease in the full width at half maximum (FHWM) and the inexistence of morphological changes in the same temperature interval. For thermal treatments performed at temperatures above 250℃, further changes in FWHM and in resistivity are negligible. However, a change in microstructure appears through void formation, indicating the onset of agglomeration. The absence of grain growth is thought to be due to the influence of the additional tin layer acting as a surface diffusion barrier. From those observations, the agglomeration phenomenon is uncoupled from the resistivity changes in the temperature range studied here.

—References—

(1) National Renewable Energy Laboratory (NREL) www.nrel.gov, retrieved 20 march 2013
(2) C.E.Kennedy, K.Terwilliger, J SOL ENERG-T ASME, pp.262-269 (2005)
(3) A.Heimsath, G.Kutscheidt, P. Nitz, SolarPaces proceedings (2011)
(4) H.C. Kim, T.L. Alford, D.R. Allee, Appl. Phys. Lett. 81, pp. 4287--4289 (2002)
(5) K.S. Gadre, T.L. Alford, J. Appl. Phys. 93, pp. 919--923 (2003)
(6) M. Hauder, J. Gstöttner, W. Hansch, D. Schmitt-Landsiedel, Appl. Phys. Lett. 78, pp. 838--840 (2001)
(7) Y. Zoo, H. Han, T.L. Alford, J. Appl. Phys. 102, pp. 083548 (2007)
(8) H.C. Kim, N.D. Theodore, T.L. Alford, J. Appl. Phys. 95, 9, pp. 5180--5188 (2004)
(9) K. Sivaramkrishnan, A.T. Ngo, S. Iyer, T.L. Alford, J. Appl. Phys. 105, 6, pp.063525 (2009)
(10) B. Schweig, Mirrors: A guide to the manufacture of mirrors and reflecting surfaces, (Pelham, London, 1973)
(11) J.F.Whitfield, Electrical craft principles, (The Institution of Electrical Engineers, London, 1995) 4th edn., vol.1, pp. 42--45
(12) H.E. Swanson, E. Tatge, Natl. Bur. Stand. (U.S.), Circ. 539, vol. 1, 23 (1953)
(13) S. Strehle, J.W. Bartha, K. Wetzig, Thin Solid Films, 517, 11, pp. 3320--3325 (2009)
(14) D. Astruc, Nanoparticles and catalysis, (Wiley Online Library, 2008) pp. 205
(15) D.J. Srolovitz, M.G. Goldiner, JOM, 47, 3, pp. 31--36 (1995)
(16) L.I. Maissel, R. Glang, Handbook of thin film technology, (McGraw-Hill, Maissel, Glang, New York, 1970)
(17) C.V. Thompson, Annu. Rev. Mater. Sci., 30, 1, pp. 159--190 (2000)
(18) S.K. Sharma, J. Spitz, Thin Solid Films, 65, 3, pp. 339--350 (1980)
(19) S.K. Sharma, J. Spitz, J. Mater. Sci. Lett., Vol.16, No.2, pp. 535--536 (1981)
(20) L.E.Murr, Interfacial phenomena in metals and alloys, (Addison-Wesley, Reading, MA, 1975)
(21) T.L. Alford, L. Chen, K.S. Gadre, Thin Solid Films, 429, 1-2, pp. 248--254 (2003)
(22) H. Han, Y. Zoo, J.W. Mayer, T.L. Alford, J. Appl. Phys., 102, 3, pp. 036101 (2007)
(23) K. Sugawara, M. Kawamura, Y. Abe, K. Sasaki, Microelectron. Eng, 84, 11, pp. 2476--2480 (2007)
(24) K. Sugawara, Y. Minamide, M. Kawamura, Y. Abe, K. Sasaki, Vac., 83, 3, pp. 610--613 (2008)